

EXPERIMENTAL STUDY OF SURFACE EFFECTS ON THE RESONANCE OF AN ACOUSTICALLY DRIVEN BUBBLE IN XANTHAN GEL

Z. Zulkefli

Dept. of Mechanical and Manufacturing Engineering, Universiti Putra Malaysia, 43400, Selangor, Malaysia

Email: zamirz@eng.upm.edu.my

ABSTRACT

Many measurement schemes have been developed to study the resonant characteristics of a bubble near a surface. The desire is to be able to measure the free field characteristics of such a bubble. For experimental investigations, a trade-off must be made between the size of the apparatus and the free field measurement. Thus there is a need to study the effect of surface interference on the resonant characteristics of a bubble. Recent works have shown that Xanthan gel is a suitable alternative to sea water when studying linear bubble dynamics. The use of Xanthan gel allows for a bubble to be freely suspended, doing away with the need to mechanically hold the bubble in place. An experiment to study the resonance frequency of an acoustically driven, freely suspended bubble near a surface in Xanthan gel is described. The resonance frequency of the bubble was generally found to not be effected by surface interference for a bubble placed more than 25 bubble radii away from a surface. Moreover, mechanically suspending a bubble in place was found not to have any discernable effect on its resonance characteristics.

Keywords: surface effects, bubble resonance, xanthan gel.

INTRODUCTION

The dynamics of bubbles have been a topic of interest for almost 100 years. In 1917, Lord Rayleigh published a paper in which he described the sound produced by boiling water in a tea kettle [1]. In 1933, Minnaert, pondering the noise caused by a babbling brook, derived what is now called the Minnaert's resonance frequency for a linear, freely oscillating bubble [2]. In 1947, a deviation in Minnaert's resonance frequency near a surface was experimentally measured by Meyer and Skudrzyk [3]. Meanwhile in 1953, Strasberg developed a theory for the pulsation of non-spherical gas bubbles using energy methods and generalized capacitance, in which he was able to predict the observed shift in the resonance frequency as a function of distance from a surface [4]. More recently, Gaunaud presented a paper discussing the scattering of a linear bubble near the surface of the ocean [5]. This was followed by Feuillade's paper in 2001 discussing acoustically coupled gas bubbles with much focus placed on the interaction of the image bubble caused by a surface [6]. In 2003, McCormick used Mie scattering to examine the effects on the linear dynamics of a bubble when suspended in Xanthan gel [7, 8].

The motivation for this paper centers on the work by McCormick and Meyer and Skudrzyk. McCormick used Mie scattering to measure the resonant characteristics of an acoustically driven bubble in the 200-500 μm range suspended in viscoelastic Xanthan gel. The experiment focused on the viscoelastic effect of Xanthan gel on the linear dynamics of bubble response. From McCormick's investigations, the bubble response was found to neglect the added static viscoelasticity of the Xanthan gel for the range of frequencies and bubble sizes used. The result showed that Xanthan gel can be used as a substitute for sea water when studying linear bubble dynamics. This result is of importance to future bubble investigations since the viscoelasticity of Xanthan gel allows freely suspended bubble to stay in place longer than when it is suspended in sea water. Interestingly, during the experiment McCormick intentionally placed the bubbles multiple bubble radii away from the walls of the acoustic test cell so as to minimize any surface effects on the bubble response. However, no substantial quantitative study on the surface effects was carried out by McCormick.

Meyer and Skudrzyk's investigation focused on the deviation of the resonance frequency of a bubble as a function of distance from a surface. Their experimental results showed clear deviations in the resonance frequency of a bubble as it was brought closer to a surface. For a rigid wall, Meyer and Skudrzyk data showed a significant drop in the resonant frequency for bubble positions closer than about 18 bubble radii away. This distance would correspond to about 0.4 to 1.0 cm in McCormick's test cell for a bubble with a radius of 2 mm.

Meyer and Skudrzyk's results suggest that surface effects may play an important role on the resonant frequency of a bubble, especially for McCormick experimental investigation.

Additionally, the experimental arrangement used by Meyer and Skudrzyk is very similar to McCormick's experimental setup. A significant difference between the two experiments is that Meyer and Skudrzyk mechanically positioned their bubbles in water using different arrangements of wires, while McCormick's bubbles were suspended in Xanthan gel without any mechanical assistance. The effects the wires had on the shape of the bubble and hence, its resonance response was not explicitly quantified by Meyer and Skudrzyk. It must be noted however, that the use of different wire arrangements clearly points to awareness by Meyer and Skudrzyk of the potential effects the mechanical intrusions might have had on their experimental results.

The purpose of experiment is to show that surface effects on the resonance frequency of an acoustically driven bubble suspended in Xanthan gel is not a measurable effect, specifically in McCormick's test cell. Furthermore, the experiment also tries to show that mechanically suspending a bubble does significantly affect its resonance frequency.

Bubble Theory

An easy way to analytically satisfy the boundary conditions for a bubble near a surface is to consider an image bubble reflected about the surface that interacts with the real bubble. For the rigid surface case, the boundary condition requires that the normal velocity at the wall tends to zero. This gives an image bubble that is in phase with the real bubble. For a pressure release surface, the boundary condition requires that the pressure at the surface goes to zero. In this case the image bubble is out of phase with the real bubble.

Following Feuillade and Twersky [6, 9], there are two approaches to solving the interaction of coupled bubbles in the time domain. They are referred to as the multiple scatter approach and the self consistent approach. For the multiple scatter approach, the radiated field from the bubble is considered to be the sum of the radiation from each multiple scatter. The radiated field consists of the driving pressure on the first bubble, the scattered field from the second bubble and progressively higher terms of the back and forth scattering between the two bubbles. A concern when using the multiple scatter approach is to ensure that the radiated field will converge. Through examination of the summation, convergence can be assured for large damping or large bubble separation.

The self-consistent approach meanwhile, considers the total radiated field to be the sum of the radiated field due to the driving pressure from the first bubble and the re-scattered field from the second bubble, which is itself the total radiated pressure field. A binomial expansion of the self-consistent solution yields the multiple scatter solution. However a distinction can be shown between the multiple scatter approach and the self-consistent approach for multiple strongly interacting bubbles.

The self-consistent approach is used to determine the relation between the resonance frequency of a bubble and its distance from the surface during this experiment. The distance between the real bubble and the imaginary bubble is defined as d and is twice the distance between the real bubble and the surface of interaction.

Following Devin [10], the equation of motion for a linear bubble when modeled as a linear oscillator is given by

$$m_D \ddot{v} + b_D \dot{v} + \kappa_D v = -P e^{-i\omega t} \quad (1)$$

where

$$m_D = \frac{\rho_l}{4\pi R_0} \quad (2)$$

$$b_D = \frac{b}{16\pi^2 R_0^4} \quad (3)$$

$$\kappa_D = \frac{3\gamma P_A}{4\pi R_0^3} \quad (4)$$

Here m_D is the effective mass of the bubble, v is the volume of the bubble, b_D is the effective damping coefficient, b is the damping coefficient, κ_D is the effective stiffness constant, ρ_l is the fluid density, R_0 is the bubble equilibrium radius, P is the driving pressure, P_A is the ambient pressure, ω is the frequency and γ is the ratio of specific heats at constant volume.

Additionally for the case of a single bubble, assuming

$$v = \bar{v} e^{-i\omega t} \quad (5)$$

then

$$\bar{v} = \frac{-P}{\kappa - \omega^2 m + i\omega b} = \frac{\frac{-P}{\omega^2 m}}{\left[\frac{\omega_0^2}{\omega^2} - 1 \right] + \frac{ib}{m\omega}} \quad (6)$$

where ω_0 is the Minnaert frequency.

For the case of two coupled bubbles, the equation of motion for each bubble has an additional forcing component due to the radiated response from the other bubble.

$$m_1 \ddot{v}_1 + b_1 \dot{v}_1 + \kappa_1 v_1 = -P_1 e^{i(\phi_1 - \omega t)} - \frac{\rho e^{ikd}}{4\pi d} \ddot{v}_2 \quad (7)$$

$$m_2 \ddot{v}_2 + b_2 \dot{v}_2 + \kappa_2 v_2 = -P_2 e^{i(\phi_2 - \omega t)} - \frac{\rho e^{ikd}}{4\pi d} \ddot{v}_1 \quad (8)$$

Where d is the distance between the center of the real bubble and the center of the image bubble. Since the bubbles being considered have to be identical, $m_1 = m_2 = m$, $b_1 = b_2 = b$ and $\kappa_1 = \kappa_2 = \kappa$.

Define

$$\frac{1}{2}(v_1 + v_2) \equiv v_+ \quad (9)$$

Adding equation (7) to equation (8) and substituting in equation (9) results in

$$\left(m + \frac{\rho e^{ikd}}{4\pi d} \right) \ddot{v}_+ + b \dot{v}_+ + \kappa v_+ = -\frac{1}{2} (P_1 e^{\phi_1} + P_2 e^{\phi_2}) e^{-i\omega t} \quad (10)$$

Similarly, by subtracting equation (8) from equation (7) and defining

$$\frac{1}{2}(v_1 - v_2) \equiv v_- \quad (11)$$

results in

$$\left(m - \frac{\rho e^{ikd}}{4\pi d} \right) \ddot{v}_- + b \dot{v}_- + \kappa v_- = -\frac{1}{2} (P_1 e^{\phi_1} - P_2 e^{\phi_2}) e^{-i\omega t} \quad (12)$$

The two quantities v_+ and v_- represent the modes of the system. For the '+' mode, the two bubbles are oscillating in phase while for the '-' mode, the bubbles are oscillating out of phase. Realizing this fact and utilizing the method of images, the '+' mode represents the rigid wall at a distance $d/2$ from the bubble and the '-' mode represents the pressure release surface at a distance $d/2$ from the bubble.

Comparing equations (10) and (12) with equation (1), it can be observed that the equations have identical forms. Therefore, by comparison with equation (6)

$$\bar{v}_\pm = \frac{-\frac{1}{2}(P_1 e^{\phi_1} \pm P_2 e^{\phi_2})}{\kappa - \omega^2 \left(m \pm \frac{\rho e^{ikd}}{4\pi d} \right) + i\omega b} = \frac{P_\pm}{\kappa - \omega^2 m_\pm + i\omega b_\pm} \quad (13)$$

Separating the denominator into real and imaginary terms, we obtain

$$m_{\pm} = m \pm \frac{\rho \cos(kd)}{4\pi d} \quad (14)$$

$$b_{\pm} = b \pm \frac{\omega \rho \sin(kd)}{4\pi d} \quad (15)$$

From equations (14) and (15), it can be seen that in the range where the near field coupling can be ignored, the effect of the surfaces is essentially to add or subtract an extra mass and damping term. At resonance, the real part of the denominator in equation (13) will go to zero. This allows the new resonance frequency to be determined. Using $\kappa = \omega_0^2 m$ and $k = \omega/c$ where c is the speed of sound, the resonant frequency can be written as

$$\omega_0^2 m = \omega_{0\pm}^2 m \pm \frac{\omega_{0\pm}^2 \rho \cos\left(\frac{\omega_{0\pm} d}{c}\right)}{4\pi d} \quad (16)$$

Notice that in equation (16) ω_0 is the resonant frequency for a bubble and $\omega_{0\pm}$ is the resonant frequency of a bubble in the presence of a boundary. Rewriting the equation gives

$$\omega_0^2 m = \omega_{0\pm}^2 m \left(1 \pm \frac{R_0}{d} \cos\left[\frac{\omega_{0\pm} d}{c}\right] \right) \quad (17)$$

The experimental interest is in the non-dimensional frequency of the bubble near a wall given by

$$\xi = \frac{\omega_{0\pm}}{\omega_0} \quad (18)$$

as a function of the non-dimensional distance to the wall. The non-dimensional distance is itself given by

$$\varepsilon = \frac{h}{R_0} = \frac{d}{2R_0} \quad (19)$$

where h is the distance from the bubble center to the surface in question.

Rewriting equation (17) in terms of non-dimensional quantities gives

$$1 = \xi^2 \left(1 \pm \frac{1}{2\varepsilon} \cos\left[\frac{2\xi\varepsilon R_0 \omega_0}{c}\right] \right) \quad (20)$$

Substituting the Minnaert frequency into the equation and after some rearrangement, equation (20) can be written in a more useful form as

$$\xi = \frac{1}{\sqrt{1 \pm \frac{1}{2\varepsilon} \cos\left(\frac{2\xi\varepsilon}{c} \sqrt{\frac{3\gamma P_A}{\rho_l}}\right)}} \quad (21)$$

Equation (21) is a transcendental equation relating ξ and ε which can be solved through iteration. This equation is used to provide a theoretical basis for the data obtained by the experiment.

Mie Scattering

Mie scattering is the scattering of electromagnetic waves by spherical inclusions. The theoretical analysis of this scattering compares directly with the scattering of acoustical waves from a sphere as given by Anderson [11] and is done by expanding incident waves into spherical harmonics and matching boundary conditions. The details of the Mie scattering procedure used for the experiment are given by McCormick [7]. However the important points for the Helium-Neon (HeNe) laser used in the experiment ($\lambda \approx 300 \mu\text{m}$) are as follows:

1. The angular dependence of scattered light intensity has little fine structure at about 80° from forward scatter.
2. The scattered intensity for small oscillations is approximately linear with radius.

This means that a laser and photo-multiplier tube system aligned at approximately 80° from forward can be used to measure the linear radius variations with time.

EXPERIMENTAL SETUP

A schematic of the setup used for the experiment is shown in Figure 1. The equipments and setup used in the experiment are the same equipments and setup used by McCormick for his work. Details of the experimental arrangement can be found in McCormick's work [7]. Suffice to say that the experimental setup consists of a circular piezoelectric transducer to acoustically vibrate the bubble under study, a test cell to hold the Xanthan gel and the bubble being studied, a HeNe laser to provide the light source, a stereo-microscope and photomultiplier tube to capture the bubble response, a vector signal analyzer to generate the needed signals and carry out preliminary analysis of the bubble response and finally a computer to store the experimental data.

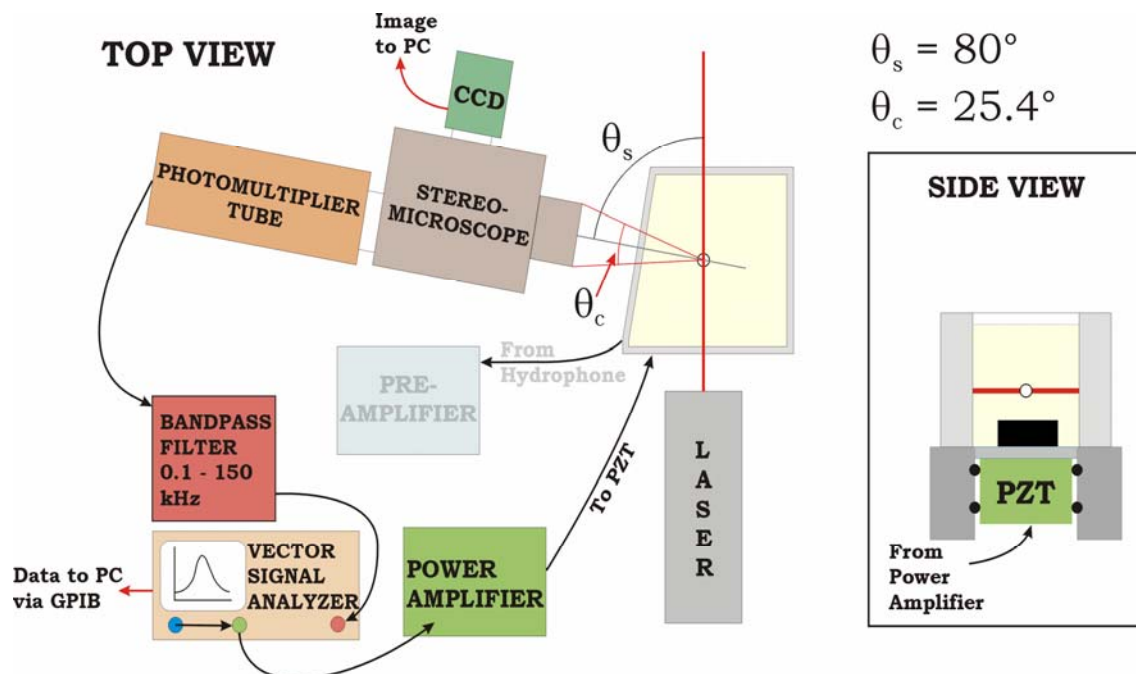


Figure 1: Schematic of experimental setup used to study surface effects on bubble resonance [7].

Minor modifications were carried out on the test cell to simplify control of the distance between the bubble and the surface of interest. Figure 2 shows an aerial view of the test cell with the modification carried out clearly visible. The modifications entailed the introduction of a sealed edge hole to the bottom of the test cell. This change enabled a piston with the required surface to be vertically maneuvered into the test cell; through the center of the circular piezoelectric actuator and the sealed edge hole. In this way, the distance between the surface of the piston and the bubble can be easily controlled. This method effectively did away with the need for recalibrating the equipments with every repositioning of the bubble in the test cell. Unfortunately, the viscoelasticity of Xanthan gel and the need to determine the test cell acoustic response at each bubble position severely limited the advantages obtained from the modifications.

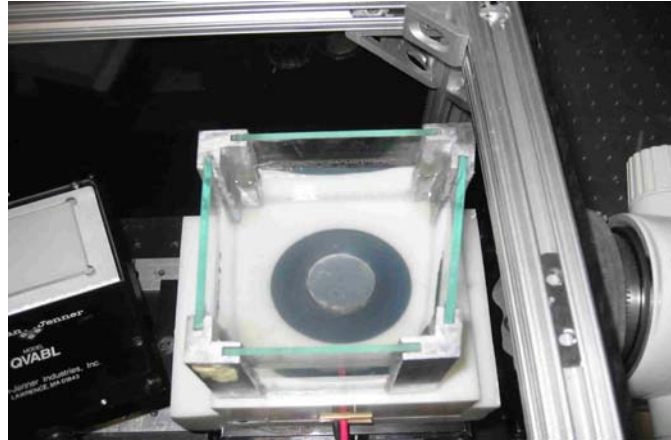


Figure 2: Aerial view of modified test cell.

Experimental Methods

When filling the test cell with Xanthan gel, care was made to ensure that the gel was free of any bubble. Unwanted bubbles were removed prior to the experiment. A bubble of the desired radius was then carefully placed into the test cell using a syringe. Care must be taken in placing the bubble so that the light scattered by the bubble is at its maximum possible intensity as viewed through the stereo-microscope while also being near enough to the surface of interest. The introduction of the piston aids in meeting these requirements since the proximity of the bubble to the surface can be changed while still keeping the bubble in an optimal position for data acquisition.

When the bubble is adequately positioned in the test cell, its size is then digitally captured and stored for later determination of its exact radius. The bubble is then acoustically driven using the piezoelectric transducer. The amplitude and frequency of the driving signal is provided by the vector signal analyzer and amplified before it reaches the piezoelectric transducer. The bubble response was then obtained by the vector signal analyzer using the stereo-microscope, photomultiplier tube and bandpass filter arrangement. Preliminary analysis of the data was then carried out before it is sent to the PC for storage and further data analysis.

The response obtained from the experiment consists of both the bubble acoustic response and the test cell acoustic response. To obtain only the bubble acoustic response, the test cell acoustic response had to also be determined. This was done by replacing the bubble with a needle hydrophone, whereby the tip of the hydrophone coincides with the position of the bubble during the experiment. The piezoelectric transducer was then turned on and the test cell acoustic response at the position of interest was then obtained.

The test cell acoustic response data was then filtered out from the original acoustic response using a Wiener filter. The Wiener filter used is the same Wiener filter used by McCormick in his investigations [7]. The important aspect of the Wiener filter relevant for this discussion is that it is a linear, time invariant filter used to minimize noise that is unrelated to the input signal. Fourier transform was used to change the response from the time domain into the frequency domain. Due to the frequency dependence of the cell response, there are certain frequencies where the amplitude of the acoustical response is very low. Division by this small amplitude would give rise to false peaks in the resultant response. To avoid this, a pre-whitening factor was introduced. The value of the pre-whitening factor used is the average value of the optical noise background present when there is no bubble in the test cell. The resulting acoustic response after Wiener filtering consists of only the sought after bubble acoustic response. This experimental procedure was carried out for different combinations of bubble size and position.

RESULTS AND DISCUSSIONS

Figure 3 shows the pressure compensated normalized bubble frequency against the normalized bubble distance from a rigid surface obtained from the experiment. The bubble frequency was normalized to the predicted, pressure compensated bubble frequency while the bubble distance was normalized to the measured bubble radius. It is noted in Figure 3 that the deviation in the bubble frequency with proximity to a rigid surface shows

the same general trend as observed by Meyer and Skudrzyk and predicted by multiple bubble theory. The experimental data however, does show clear discrepancies with both Meyer and Skudrzyk's observations and the predicted values. These discrepancies for the most part are between 3 to 5 percent of the predicted value and are attributed to optical signal-to-noise issues not encountered by McCormick. Specifically, for this experiment the bubble is required to be placed near the piston which is at the center of the test cell. This resulted in the bubble being further away from the camera than in McCormick's experiment; consequently resulting in lower quality data. Additionally, the introduction of a piston into the test cell presented an additional source of extraneous vibrations especially at high enough amplitude. This in turn caused significant deviations in the observed bubble frequency near a rigid surface.

Figure 3 also allows for an easy comparison between the predicted resonant characteristics near a rigid surface and Meyer and Skurzyk's experimental data. It can be observed from Figure 3 that there is less than 1 percent deviation in the resonance frequency observed by Meyer and Skudrzyk from theory for a normalized distance of more than 25 bubble radii away. Hence, for a normalized distance of more than 25 bubble radii away, there is no measurable surface interference effect on the bubble resonant characteristics. For a normalized distance of less than 25 bubble radii, there is around 1 to 2 percent deviation in the bubble frequency observed by Meyer and Skudrzyk and theoretical predictions. This fact shows that according to multiple bubble theory, Meyer and Skudrzyk's method of mechanically holding a bubble in place did not affect the deviation in the resonance frequency of a bubble near a rigid surface.

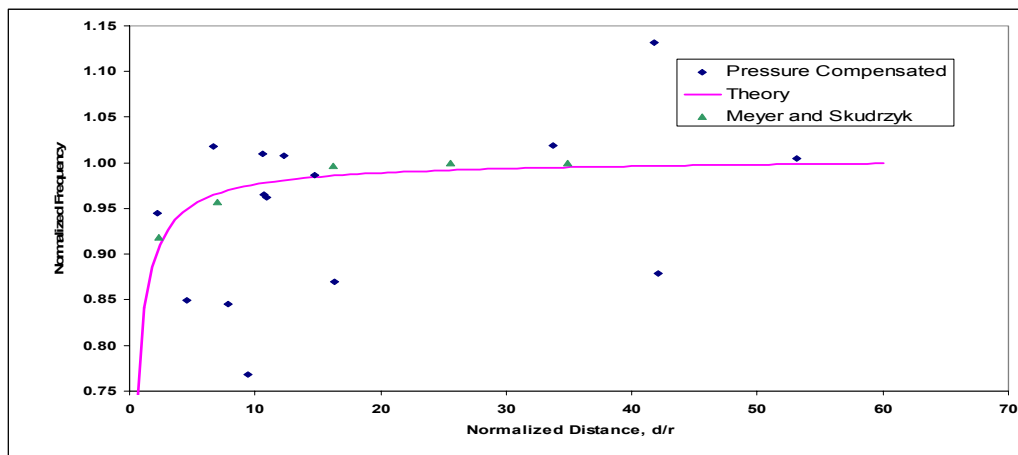


Figure 3: Graph of the normalized bubble frequency against normalized bubble distance from a rigid surface.

Figure 4 shows the pressure compensated normalized bubble frequency against the normalized bubble distance from a pressure release surface. Again, the bubble frequency was normalized to the predicted, pressure compensated bubble frequency while the bubble distance was normalized to the measured bubble radius. It is noted in Figure 4 that the deviation in the bubble frequency with proximity to a pressure release surface shows the same general trend as observed by Meyer and Skudrzyk and predicted by multiple bubble theory. The experimental data however, does show clear discrepancies with both Meyer and Skudrzyk's observations and the predicted values. These discrepancies for the most part are between 1 to 3 percent of the predicted value and are attributed to the same signal-to-noise issues encountered for the rigid surface case.

Figure 4 also allows for an easy comparison between the predicted resonant characteristics near a pressure release surface and Meyer and Skudrzyk's experimental data. It can be observed from Figure 4 that there is less than 1 percent deviation in the resonance frequency observed by Meyer and Skudrzyk from multiple bubble theory for a normalized distance of more than 14 bubble radii away. Hence, for a normalized distance of more than 14 bubble radii away, there is no measurable surface interference effect on the bubble resonant characteristics. For a normalized distance of less than 14 bubble radii, there is around 1 percent deviation in the bubble frequency observed by Meyer and Skudrzyk and theoretical predictions. This fact shows that according to multiple bubble theory, Meyer and Skudrzyk's method of mechanically holding a bubble in place did not affect the deviation in the resonance frequency of a bubble near a pressure release surface. Nevertheless for a normalized distance less than 10 radii Meyer and Skudrzyk's data predicted less deviation in the resonance frequency than predicted by multiple bubble theory.

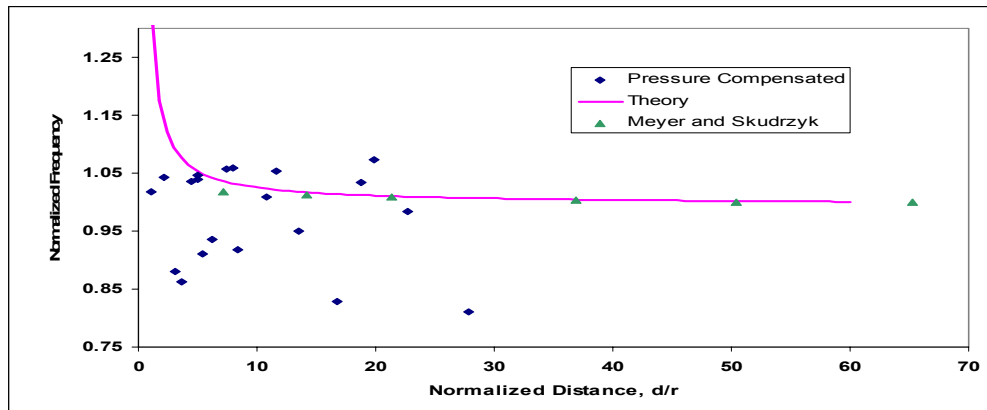


Figure 4: Graph of normalized bubble frequency against normalized bubble distance from a pressure release surface.

CONCLUSIONS

In conclusion, it has been generally observed through the experiment that the proximity of an acoustically driven bubble near a surface does not have any measurable effect on the resonant characteristics of the bubble for a distance of more than 25 bubble radii away. Instead, the experiment suggests that signal-to-noise issues in the experimental setup to be more important than surface interference effects. Additionally, the experiment was unable to conclusively show that there are no observed significant differences in the resonance frequency of a bubble when it is mechanically suspended in place and when the bubble is freely suspended. Analysis of previous works and theory suggest that there is no significant difference in the resonant characteristics of a bubble when mechanical means was used to hold a bubble in position. Further investigations should be carried out to confirm the conclusions stated here. Particular attention should be paid on the bubble resonance frequency for normalized bubble distance of less than 10 bubble radii.

ACKNOWLEDGEMENT

The authors would like to acknowledge Dr. Ronald A. Roy for inspiring and guiding this study. This work was carried out at Boston University and was partially supported by the Aerospace and Mechanical Engineering Department at Boston University.

REFERENCES

- [1] Lord Rayleigh. (1917) On the pressure developed in a liquid during the collapse of a spherical cavity. *Philosophical Magazine*, **34**: 94-98.
- [2] Minnaert, M. (1933) On musical air-bubbles and the sound of running water. *The London, Edinburgh, and Dublin Philosophical Magazine and Journal of Science*, **16**(7): 235-248.
- [3] Meyer E. and Skudrzyk, E. (1947) Sound absorption of gas bubbles. Chapter 2, *NavShips Publication 900164*, Bureau of Ships, U.S. Department of the Navy, Washington, D.C.
- [4] Strasberg, M. (1953) The pulsation frequency of non-spherical gas bubbles in liquids. *J. Acoust. Soc. Am.*, **25**(3): 536-537.
- [5] Gaunaurd, M. (1992) Acoustic scattering by an air bubble near the sea surface. *J. Oceanic Eng.*, **20**: 285-292.
- [6] Feuillade, C. (2001) Acoustically coupled gas bubbles in fluids: Time domain phenomena. *J. Acoust. Soc. Am.*, **109**(6): 2606-2615.
- [7] McCormick, R.D. (2002) Experimental investigation of linear bubble dynamics in a viscoelastic xanthan gel. *Engineering, Mechanical*, Boston University.
- [8] McCormick, R.D. and Roy, R.A. (2001). Measurements of the frequency- and size-dependent response of single, acoustically driven bubble in a polymer gel. *J. Acoust. Soc. Am.*, **110**: 27-33.
- [9] Twersky, V. (1962) Multiple scattering by arbitrary configurations in three dimensions. *J. Math. Phys.*, **3**: 83-91.
- [10] Devin, C. Jr, (1959) Survey of thermal, radiation, and viscous damping of pulsating air bubbles in water. *J. Acoust. Soc. Am.*, **31**(12): 1654-1667.
- [11] V.C. Anderson (1950). Sound scattering from a fluid sphere. *J. Acoust. Soc. Am.*, **22**(4): 426-431.